Acoustic studies of the large scale ocean circulation

Detailed knowledge of ocean circulation and its transport properties is prerequisite to an understanding of the earth's climate and of important biological and chemical cycles. Results from two recent experiments, THETIS-2 in the Western Mediterranean and ATOC in the North Pacific, illustrate the use of ocean acoustic tomography for studies of the large scale circulation. The attraction of acoustic tomography is its ability to sample and average the large-scale oceanic thermal structure, synoptically, along several sections, and at regular intervals. In both studies, the acoustic data are compared to, and then combined with, general circulation models, meteorological analyses, satellite altimetry, and direct measurements from ships. Both studies provide complete regional descriptions of the time-evolving, three-dimensional, large scale circulation, albeit with large uncertainties. The studies raise serious issues about existing ocean observing capability and provide guidelines for future efforts.

Acoustic studies of the large scale ocean circulation

Dimitris Menemenlis
dimitri@pacific.jpl.nasa.gov
Jet Propulsion Lab
California Institute of Technology
Mail Stop 300-323
Pasadena CA 91109-8099

Popular version of paper 3aA0b
Presented Wednesday morning, March 17, 1999
ASA/EAA/DAGA '99 Meeting, Berlin, Germany

The ocean stores and transports vast quantities of heat, fresh water, carbon, and other materials, and its circulation plays an important role in determining both the Earth's climate and fundamental processes in the biosphere. Understanding the development of climate and important biological cycles therefore requires detailed knowledge of ocean circulation and its transport properties. That in turn requires observing and modeling a global scale turbulent flow field so as to adequately depict its complex temporal and spatial evolution. Studying climate-scale variability is very difficult, however, because it is masked by an intense 100 km spatial scale variability (the so-called mesoscale) as well as higher frequency internal waves. Two recently developed observational methods, satellite altimetry and acoustic tomography are especially suitable for detecting climate-scale changes because they provide large-scale averages.

Satellite altimetry depends on the travel time of radio waves reflected at the sea surface to measure the sea surface elevation relative to the geoid, that is, relative to the particular gravitational equipotential to which the sea surface would conform if it were at rest with no forces acting on it. Changes in elevation result from local exchange of mass and heat with the atmosphere through the sea surface and from lateral water movements. In general terms, surface elevation and its slope provide a dynamical surface boundary condition on the general circulation.

The second observational system, ocean acoustic tomography, relies on the travel time of sound waves through the (electromagnetically opaque) ocean interior. Tomography integrates the oceanic state along many paths through a volume of fluid by transmitting sound pulses from sources to receivers. Perturbations in travel time of acoustic pulses are dominated by temperature perturbations. Hence acoustic tomography can act as a large scale ocean thermometer and provide accurate measurements of heat content, an important climate variable.

The combined power of these two technologies for studying the large scale circulation has been demonstrated in two recent experiment, THETIS-2 in the Western Mediterranean and ATOC in the North Pacific. In both experiments, the altimetric and acoustic data are combined with general circulation models, meteorological analyses, and direct measurements from ships. These model/data combinations provide regional descriptions of the time-evolving state of the ocean which are more complete and accurate than either the model or the data alone. They are an analogue of what is required globally to address various climate related questions, for initializing seasonal to interannual climate predictions, as well as for navigation and exploration purposes.

Figure Captions:

Figure 1: Study area for the THETIS-2 experiment in the Western Mediterranean. The colored contours indicate sea surface height change in centimeters between March and September 1994 from the TOPEX/POSEIDON altimeter. The black lines are acoustic tomography sections. The sea surface height increase from March to September is indicative of seasonal warming but includes complex contributions from changes in wind forcing, from evaporation and precipitation, from river runoff, and from flows through the Straits of Sicily and Gibraltar. Acoustic tomography and a numerical model of the circulation are used to separate the respective contributions to sea level anomaly.

Figure 2: The ATOC acoustic array (black lines) is superimposed on a map indicating sea surface height variability in centimeters obtained from TOPEX/POSEIDON altimetric measurements. About half of the sea surface height variability represents seasonal thermal changes within the ocean. But changes in sea surface height also include complex contributions from other processes, with the acoustic data providing a stable spatial average of heat content which it is otherwise difficult to obtain.

Figure 3: This figure illustrates results from a model/data combination which permits a complete description of the time evolving state of the ocean. The colored contours indicate temperature change averaged over the top 4000-m, from January 1996 to January 1997 (white regions indicate depths less than 4000-m). The arrows indicate the corresponding change in velocity at 610-m, the largest change being about 5 cm/s. This type of results are being used to study the large scale ocean circulation and to understand the role of the oceans in climate and climate change.

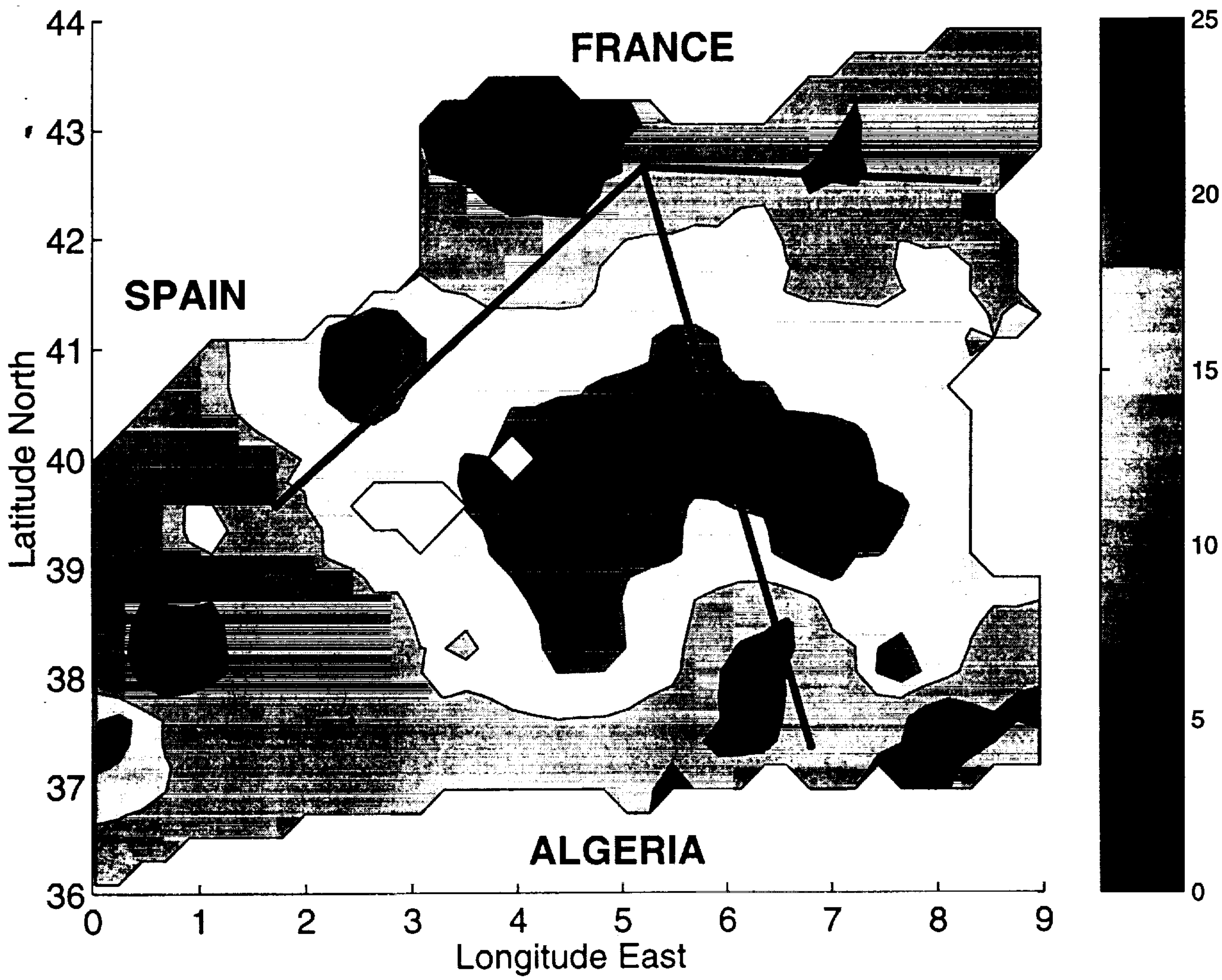
FRANCE
SPAIN
ALGERIA
Latitude North
Longitude East
44
43
42
41
40
39
38
37
36
0
1
2
3
4
5
6
7
8
9
25
20
15
10
5
0

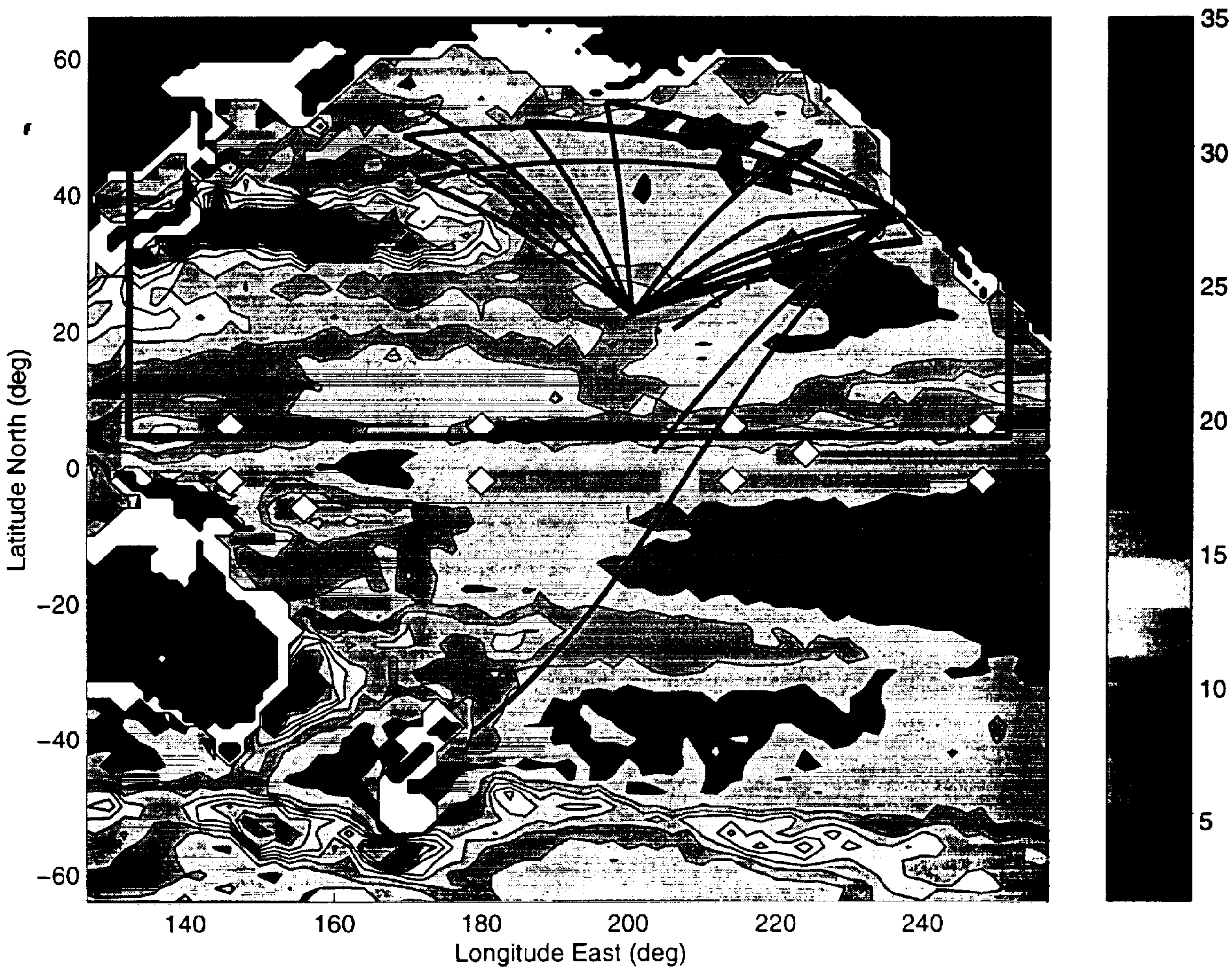

Latitude North (deg)
60
40
20
0
-20
-40
-60
140
160
180
200
220
240
Longitude East (deg)
35
30
25
20
15
10
5

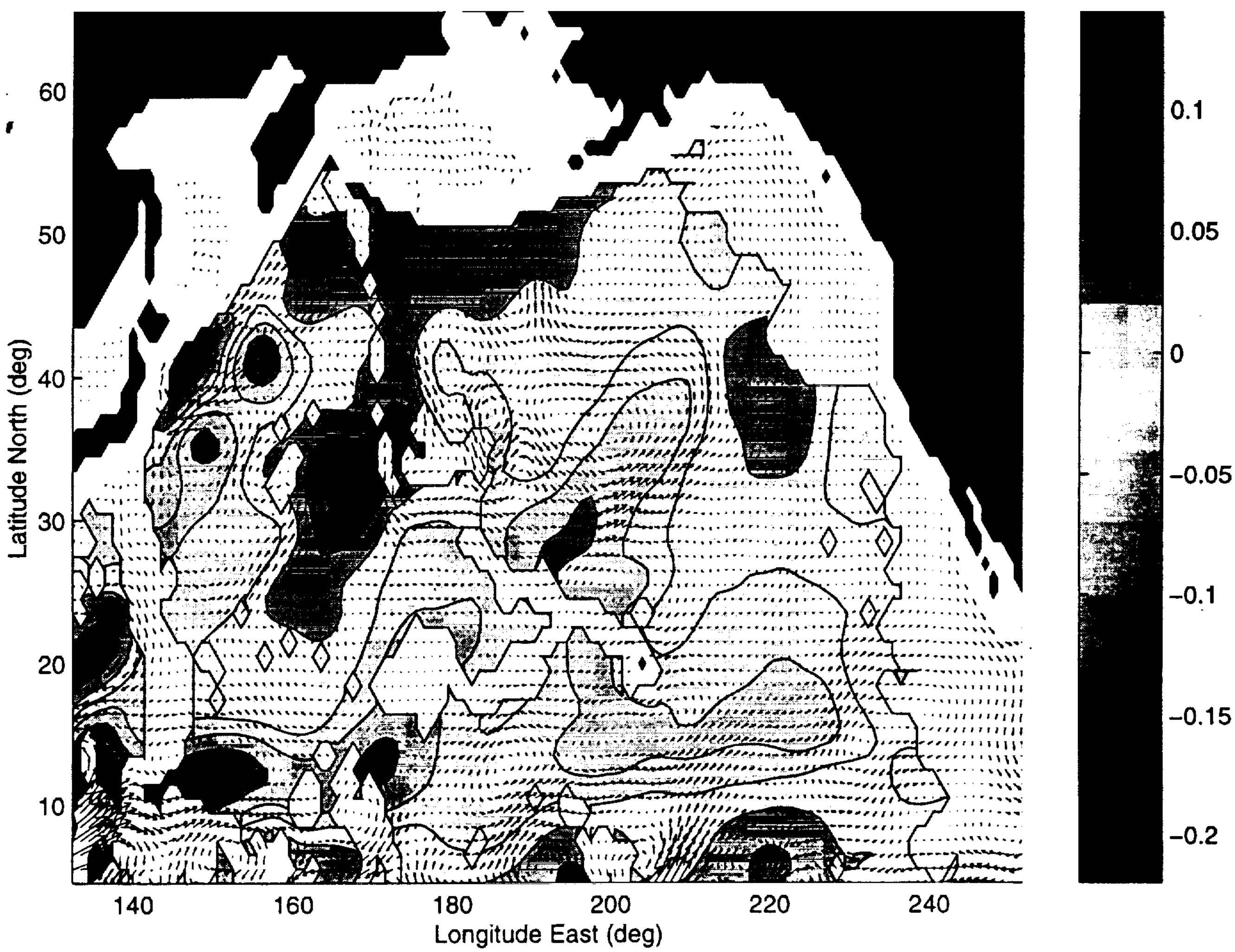

60
50
40
30
20
10
Latitude North (deg)
140
160
180
200
220
240
Longitude East (deg)
0.1
0.05
0
−0.05
−0.1
−0.15
−0.2

estimating baroclinic errors in OGCMs

using ATOC

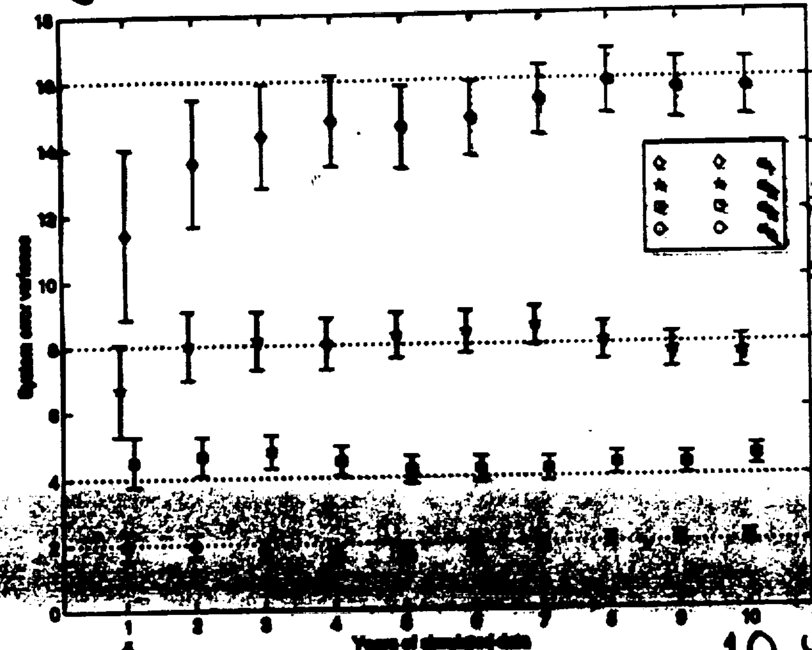

Figure 4. Estimates of system error variance based on the lag-1 difference sample covariance, $\hat{D}_1$, for simulated acoustic tomography data. Dotted lines indicate the values of $\alpha_1 \ldots \alpha_4$ used to generate the data. The error bars represent the standard error of the estimates. The figure demonstrates the increasing accuracy of the algorithm with increasing number of measurements.

using POSEIDON

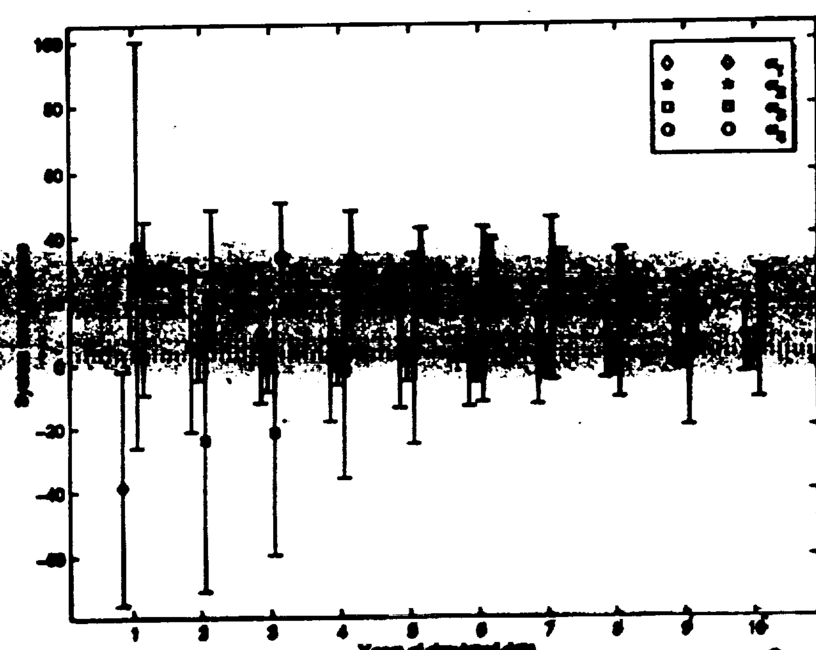

Figure 5. Estimates of system error variance based on the diagonal elements of $\hat{D}_1$ for simulated altimeter data. Dotted lines indicate the prior variances used to generate the data. Error bars represent the standard uncertainty of the estimates and they can be compared to those of Fig. 4 which were created using simulated acoustic data. The large error bars associated with the altimetric estimates suggest that altimeter data are ill-suited to the estimation of baroclinic GCM errors.

(Chechelnitsky and Menemenlis '99)

1. THETIS-2 experiment
(Western Mediterranean)

[redacted]

3. Global-ocean data assimilation system
(SCRIPPS, MIT, JPL effort)

[redacted]

Global-ocean data assimilation system

(SCRIPPS, MIT, JPL effort)

Objective

Estimate global time-evolving ocean circulation by combining modern large scale data sets and general circulation models.

Science Goals

Understand the basic state of the ocean, [redacted]

Estimate meridional fluxes and flux divergences of heat, fresh water, carbon, and nutrients.

Study global physical processes linking ocean with changing atmosphere, and their role in climate variability.

PRESENT STATUS

completed

2°, 20-level, 1-year adjoint model computation

[redacted]

(Fukumori et al., in press)

underway

1°, 20-level, 5-year adjoint model computation

1° → 1/3°, 46-level, KPP, GM forward integration

[redacted]

1985 - 2000 optimization, eventually at 1/4° global.

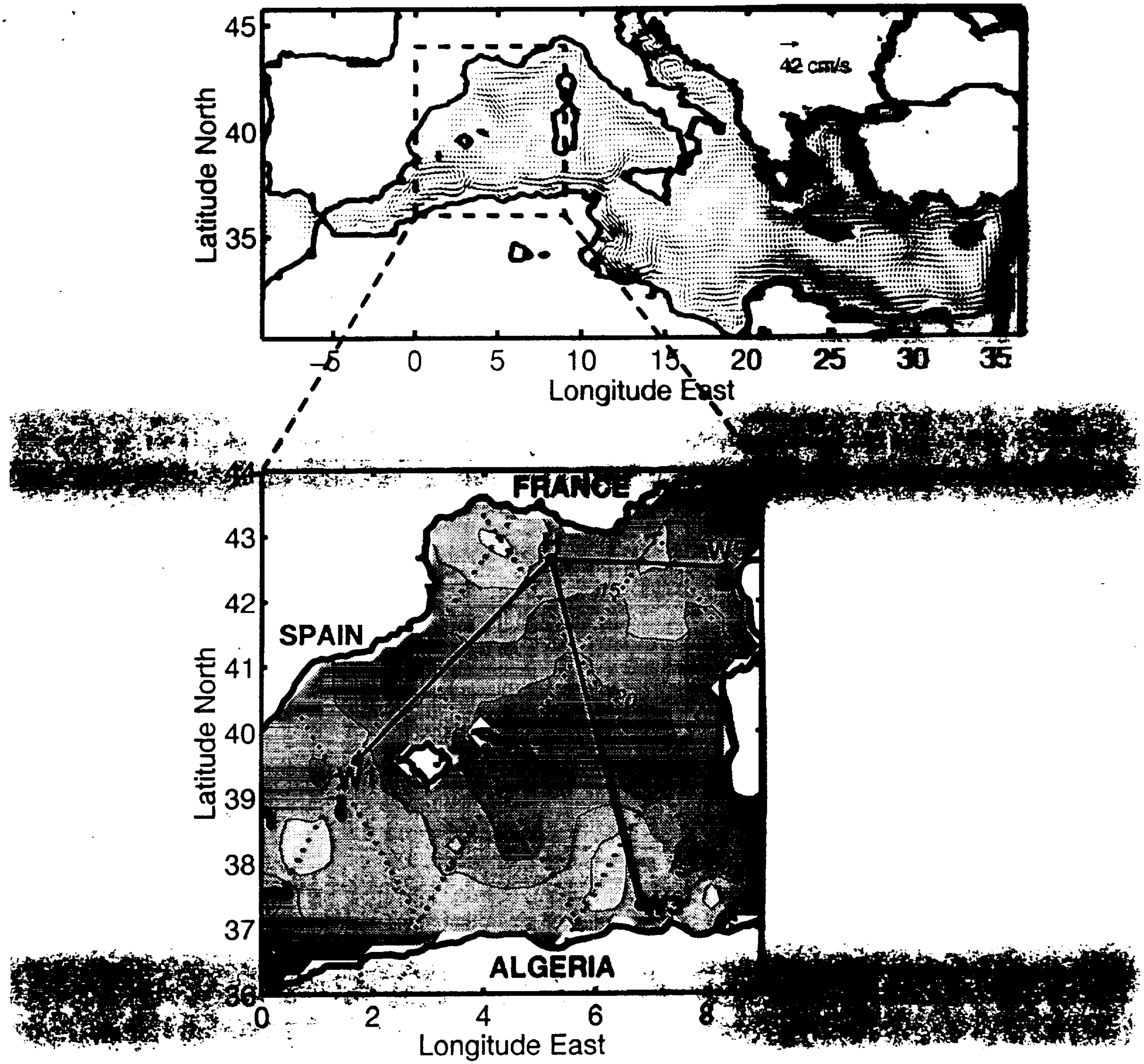

(Menemenlis et al. '97)

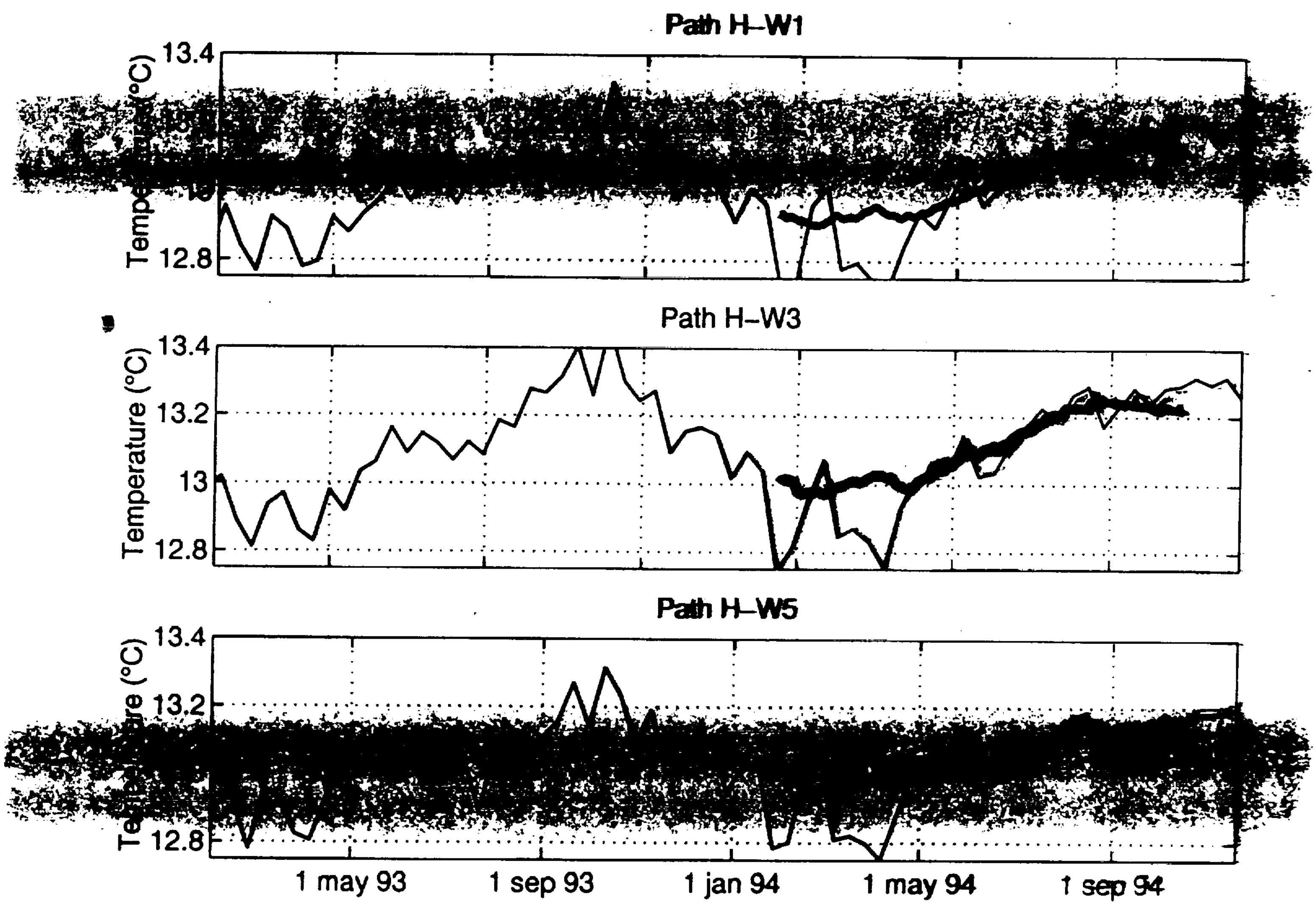

(Menemenlis et al. '97)

Estimation problem

GCM errors:

[redacted]

$$\mathbf{p}(t+1) = \mathbf{A}\,\mathbf{p}(t) + \mathbf{q}(t)$$

Measurements:

$$\mathbf{y}_{\text{data}}(t) = \mathbf{H}(t)\,\mathbf{x}_{\text{ocean}}(t) + \mathbf{r}(t)$$

Residuals:

$$\begin{aligned}\mathbf{y}(t) &= \mathbf{H}(t)\,\mathbf{x}_{\text{GCM}}(t) - \mathbf{y}_{\text{data}}(t)\\ &= \mathbf{H}(t)\,\mathbf{p}(t) - \mathbf{r}(t)\end{aligned}$$

Covariance matrices:

[redacted]

Cost function:

$$\mathbf{J} = \mathbf{p}^T(0)\mathbf{P}^{-1}\mathbf{p}(0) + \sum_t \left[\mathbf{r}^T(t)\mathbf{R}^{-1}\mathbf{r}(t) + \mathbf{q}^T(t)\mathbf{Q}^{-1}\mathbf{q}(t)\right]$$

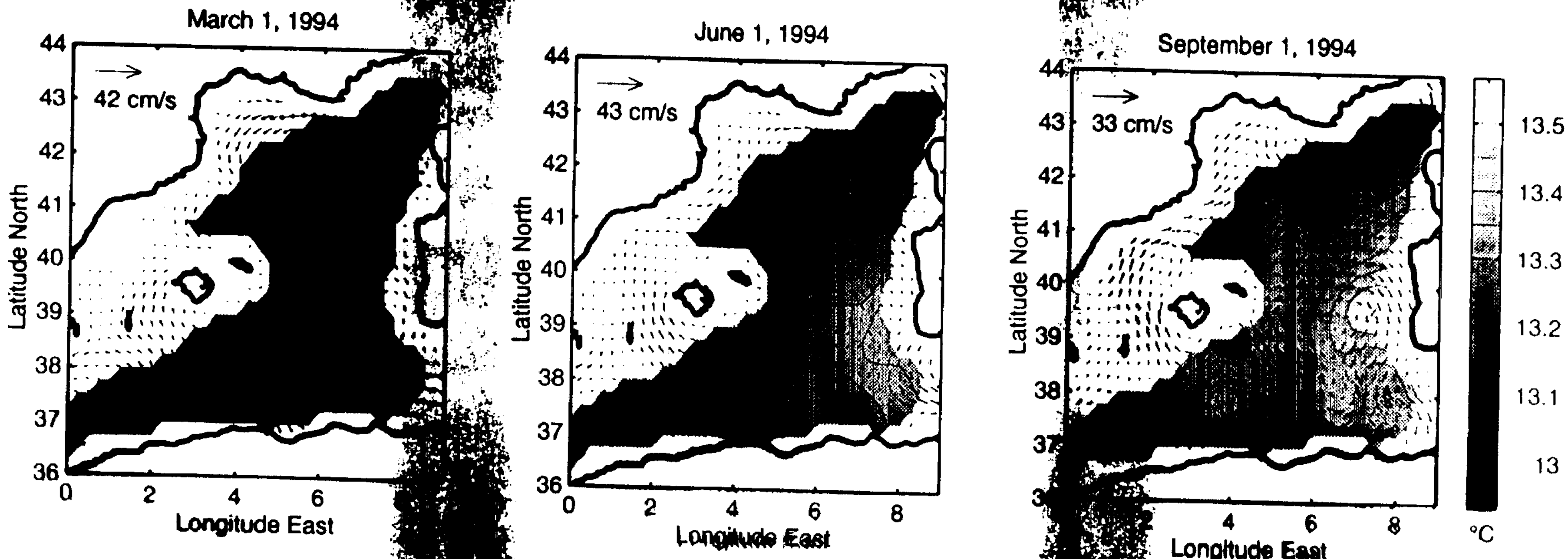

(…enlis et al. '97)

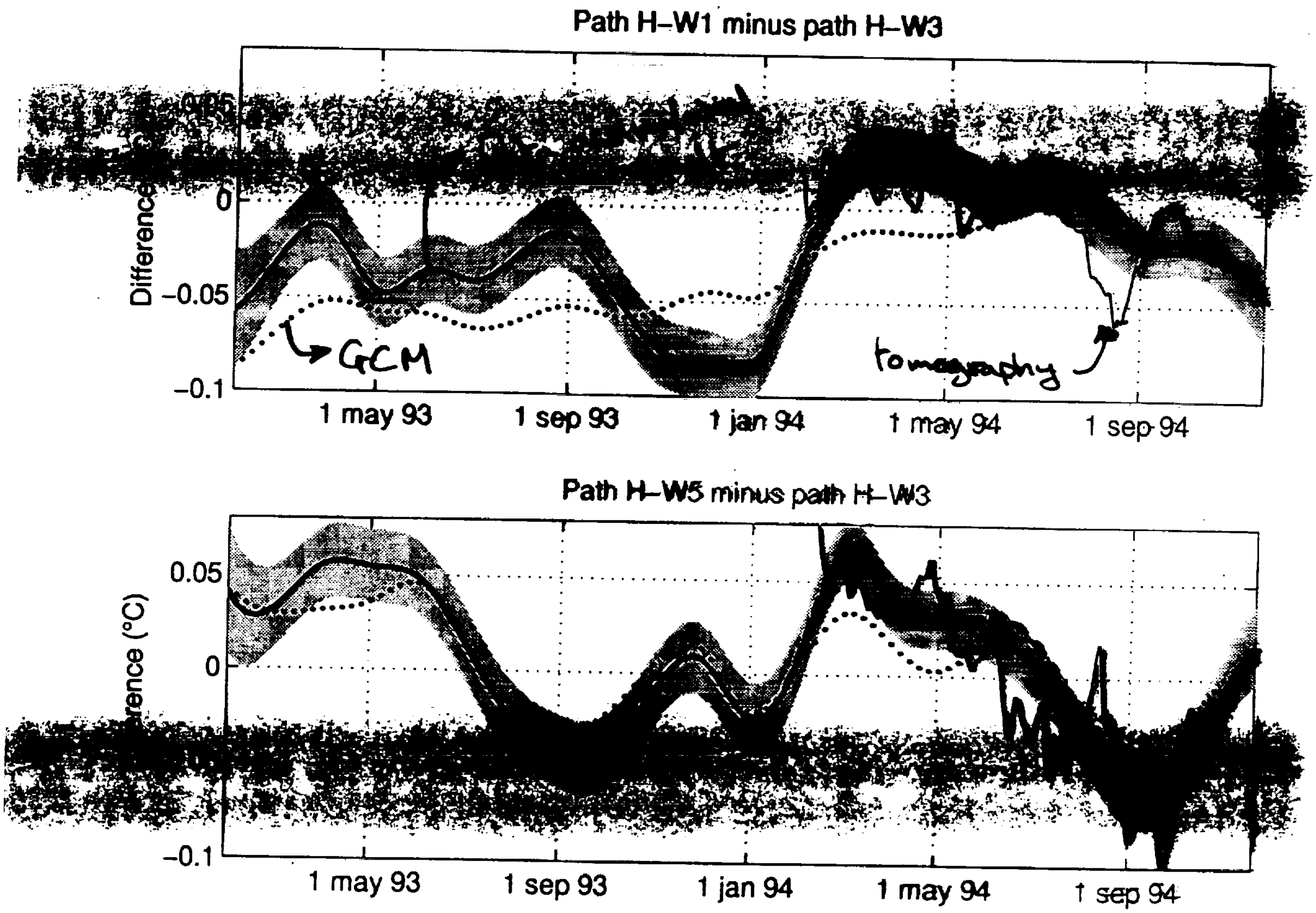

(Menemenlis et al. 97)

rms difference between
η_{altim} and η_{acoust} : 2.4 cm

rms difference between [illegible]

Table 1. Annual harmonic amplitude (in centimeters) and, in parentheses, phase [illegible]

Component	Acoustic section				
	l	k	n	o	vT
η_{clim}	2.5 (273)	2.9 (291)	2.1 (284)	2.0 (277)	2.5 (272)
η_{acoust}	2.9 (255)	2.5 (257)	2.0 (270)	2.3 (302)	0.8 (59)
η_{XBT}					2.7 (304)
η_{GCM}	2.5 (262)	3.3 (266)	1.7 (287)	1.0 (270)	0.7 (278)
η_{altim}	4.0 (271)	4.9 (276)	4.0 (281)	3.6 (275)	3.6 (282)

(The ATOC Consortium '98)

Kinetic energy

Log$_{10}$ of depth-average kinetic energy per unit mass

% barotrop mode

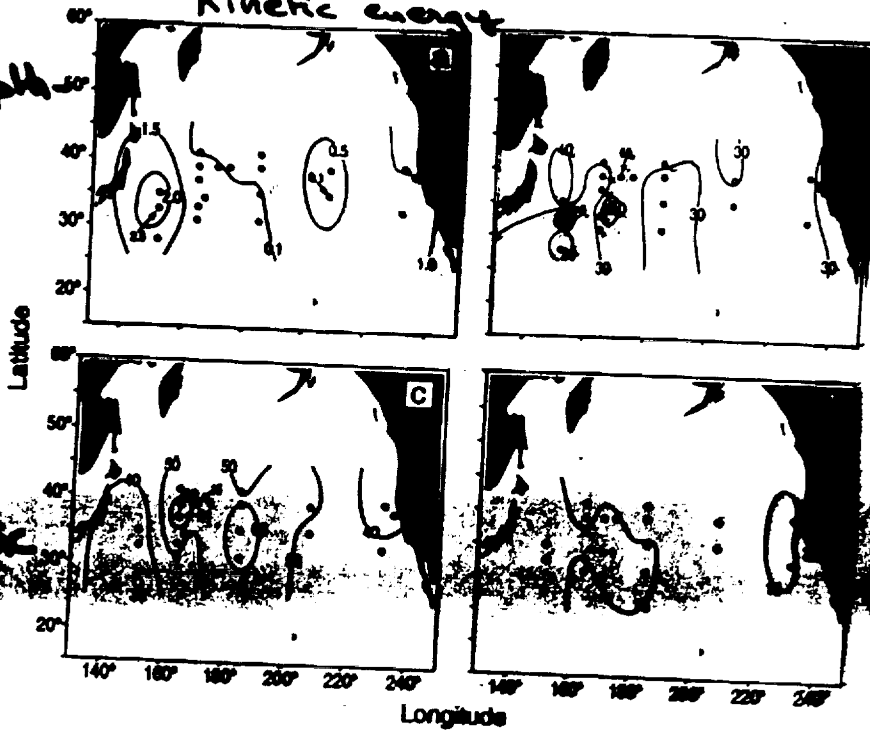

% baroclinic mode

% mode

FIG. 5. (a) Log$_{10}$ of the water column average kinetic energy per unit mass in the North Pacific Ocean. (b) Percentage of water column average kinetic energy per unit mass found in the barotropic mode. (c) Percentage of water column average kinetic energy per unit mass found in the first baroclinic mode. (d) Percentage of water column average kinetic energy per unit mass found in the second baroclinic mode.

log$_{10}$ of surface kinetic energy per unit mass

% barotropic mode

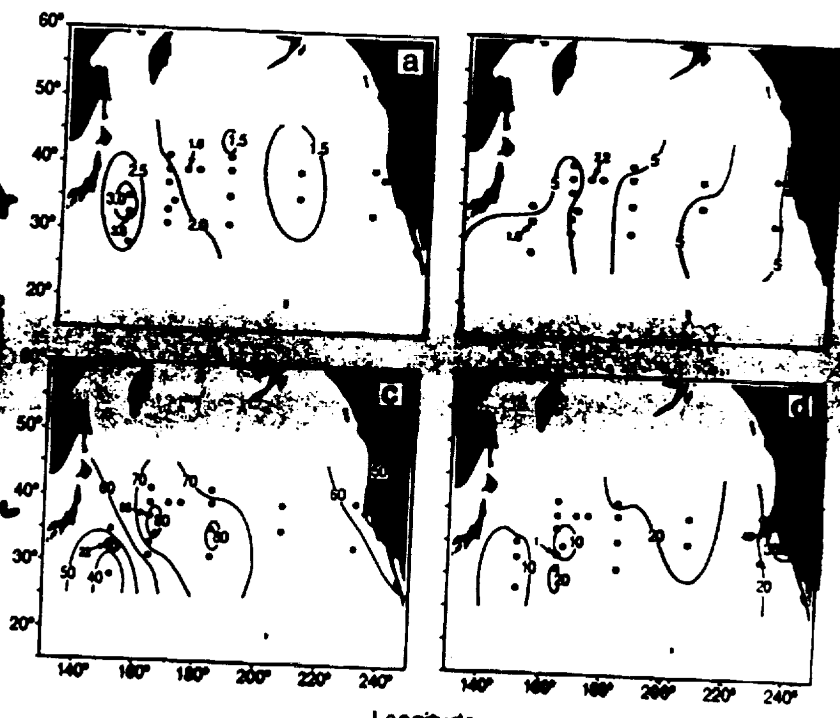

% first baroclinic mode

% second baroclinic mode

FIG. 6. (a) Log$_{10}$ of estimated surface kinetic energy per unit mass. (c–d) Same as in Fig. 5c–d except for the surface kinetic energy per unit mass $\overline{T^{(n)}}(0)$. Owing to the surface intensification of the baroclinic modes, little of the surface kinetic energy is barotropic.

(Wunsch '97)

Gilson, Roemmich, Cornuelle & Fu, in pre

SALT ANOMALY

16 X Pacific cruises over 4 years

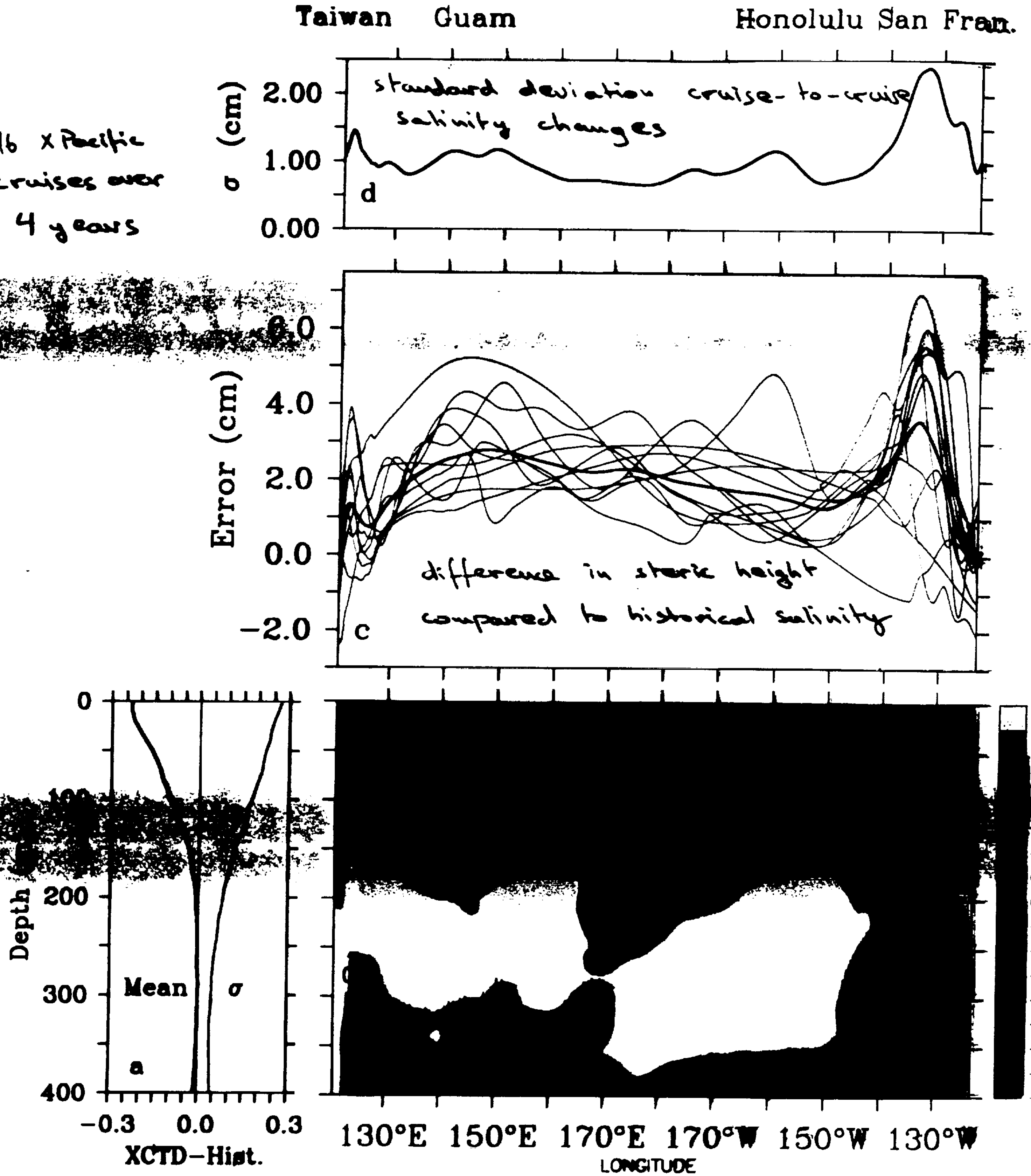

Salinity difference compared with historical data

(Gilson et al. '97)

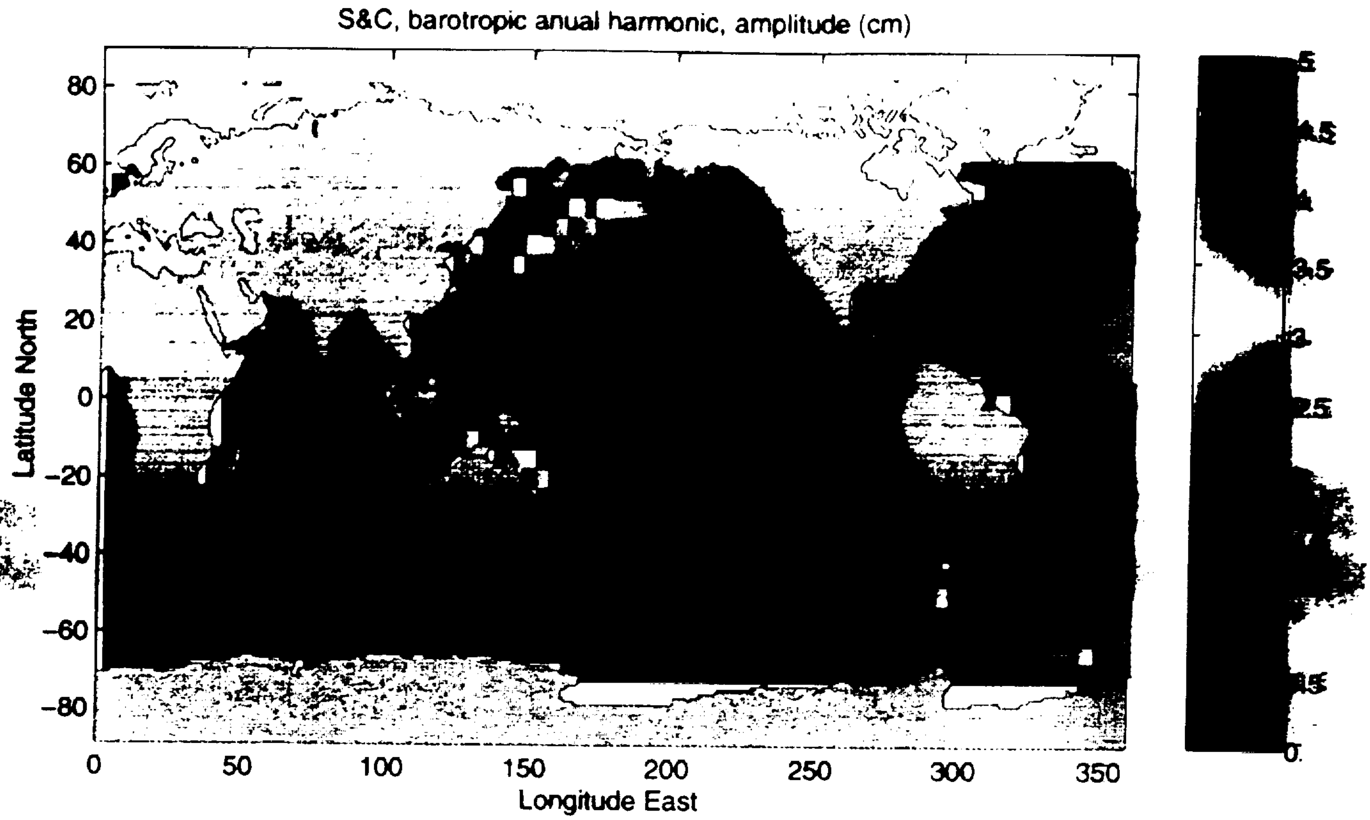
S&C, barotropic anual harmonic, amplitude (cm)
Latitude North
Longitude East
80
60
40
20
0
-20
-40
-60
-80
0
50
100
150
200
250
300
350

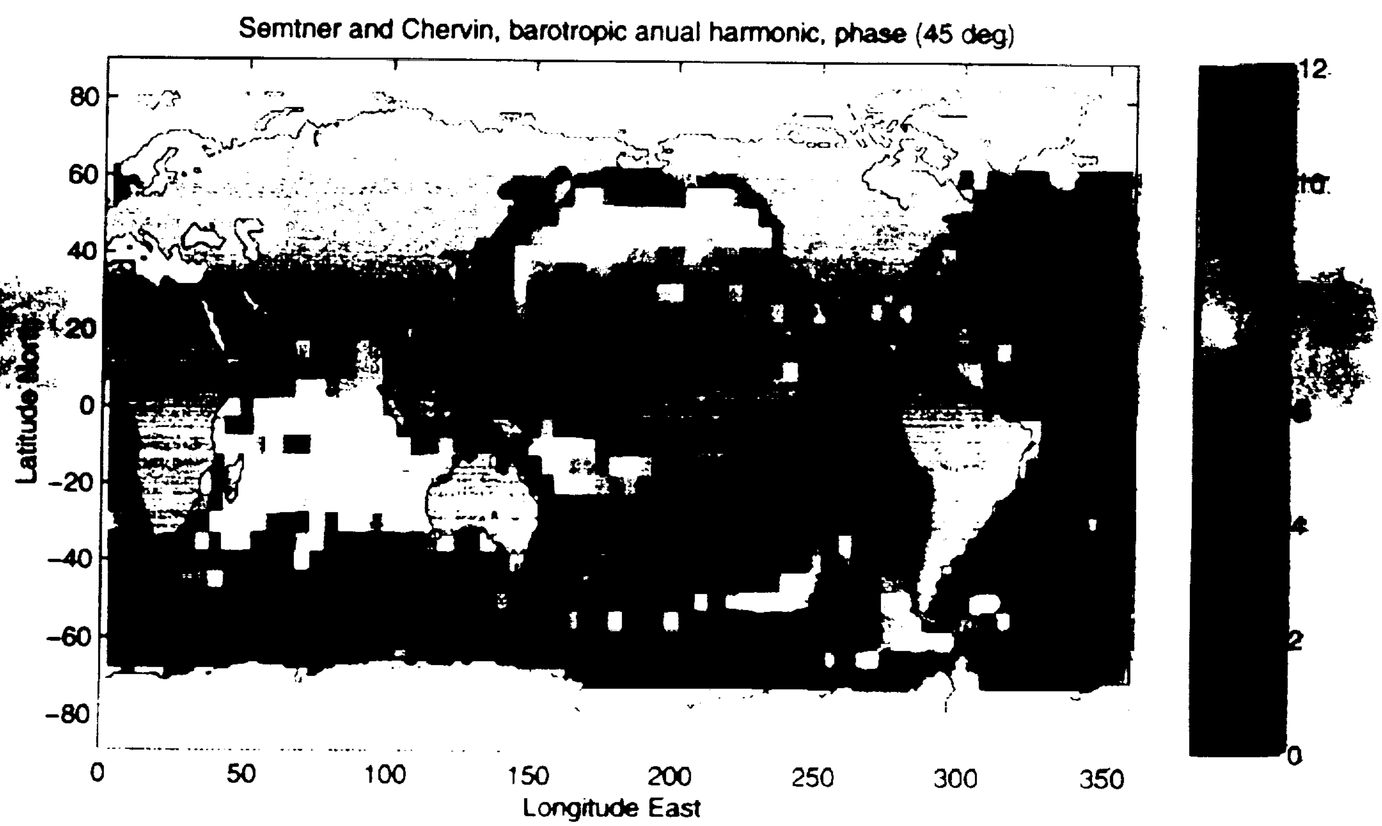
Semtner and Chervin, barotropic anual harmonic, phase (45 deg)
Latitude North
Longitude East
80
60
40
20
0
-20
-40
-60
-80
0
50
100
150
200
250
300
350
12
10
4
2
0

$$\Delta M_{ocean} + \Delta M_{water\ vapor} + \Delta M_{continental\ water} = 0$$

	amplitude (cm)	Maximum
TOPEX/POSEIDON	4.6	Sept. 27
Levitus steric	5.0	March 12
Sea level − steric	9.5	Sept 19
NCEP Atmospheric water vapor	2.0	Dec. 4
[illegible]	6.3	[illegible]
[illegible]	[illegible]	[illegible]

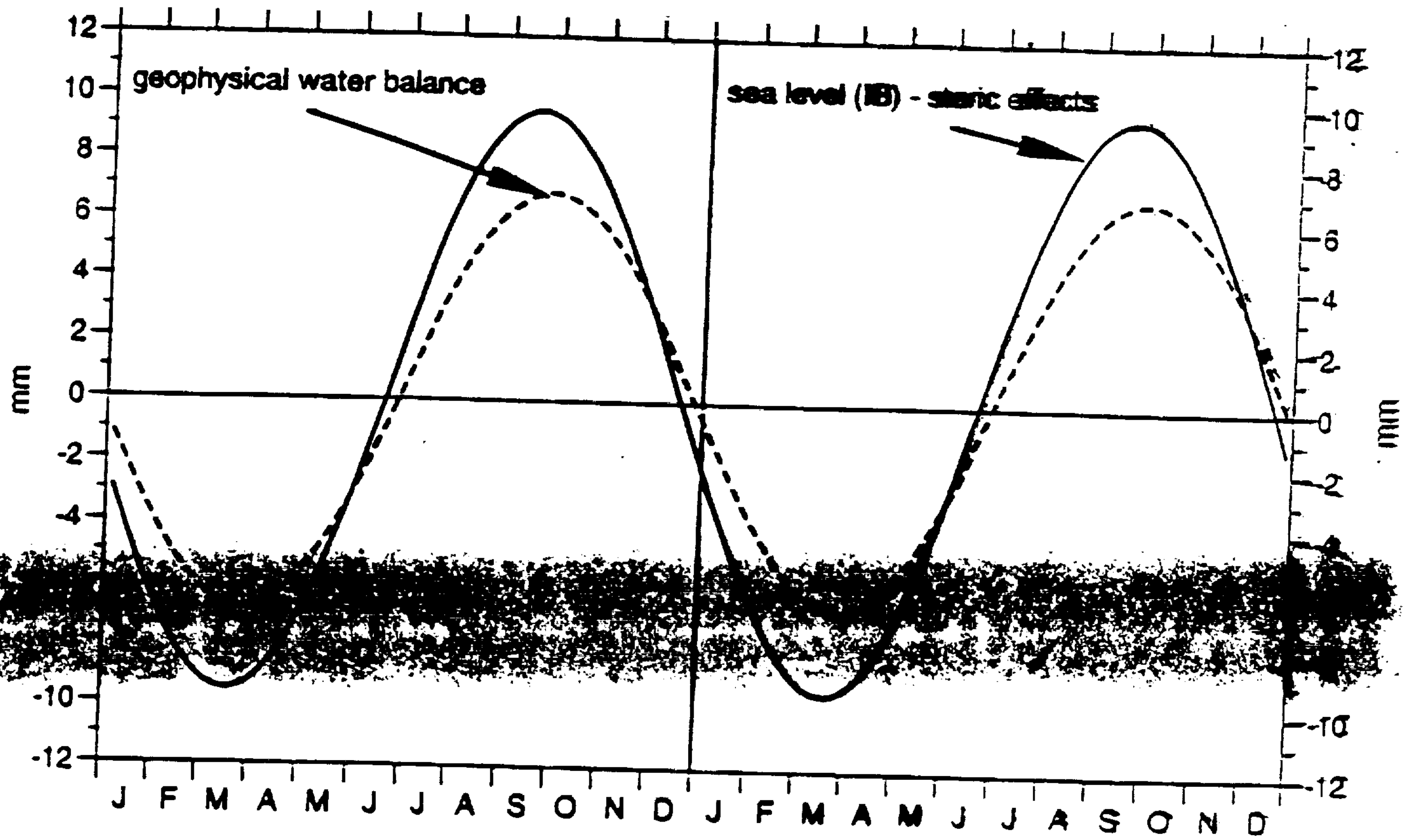

(Minster et al. 1998)

Fig. 5

January 97 — January 96

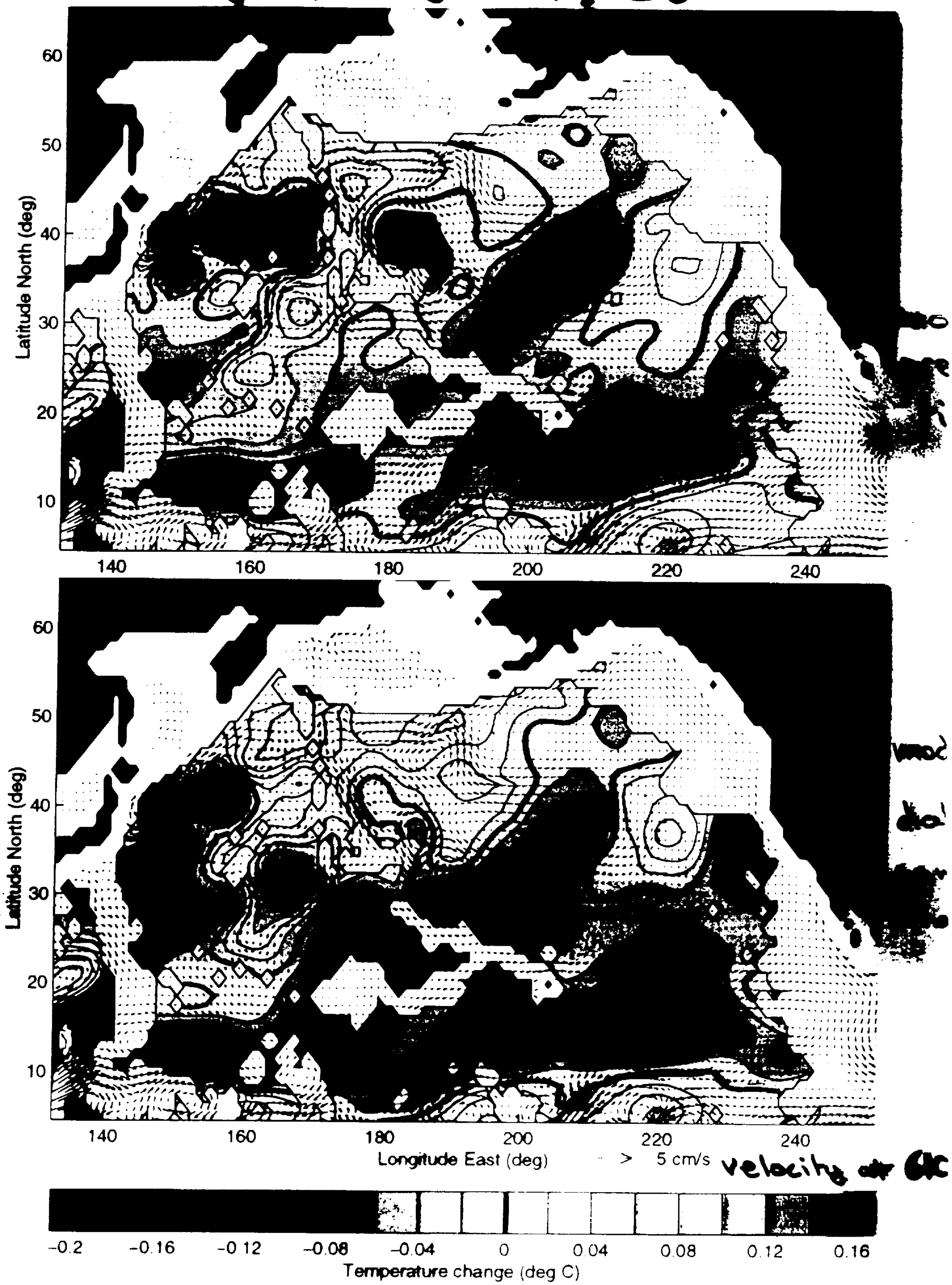

Heat content change in top 4000 m

Heat content change in 168°-240°E 16°-56°N box.

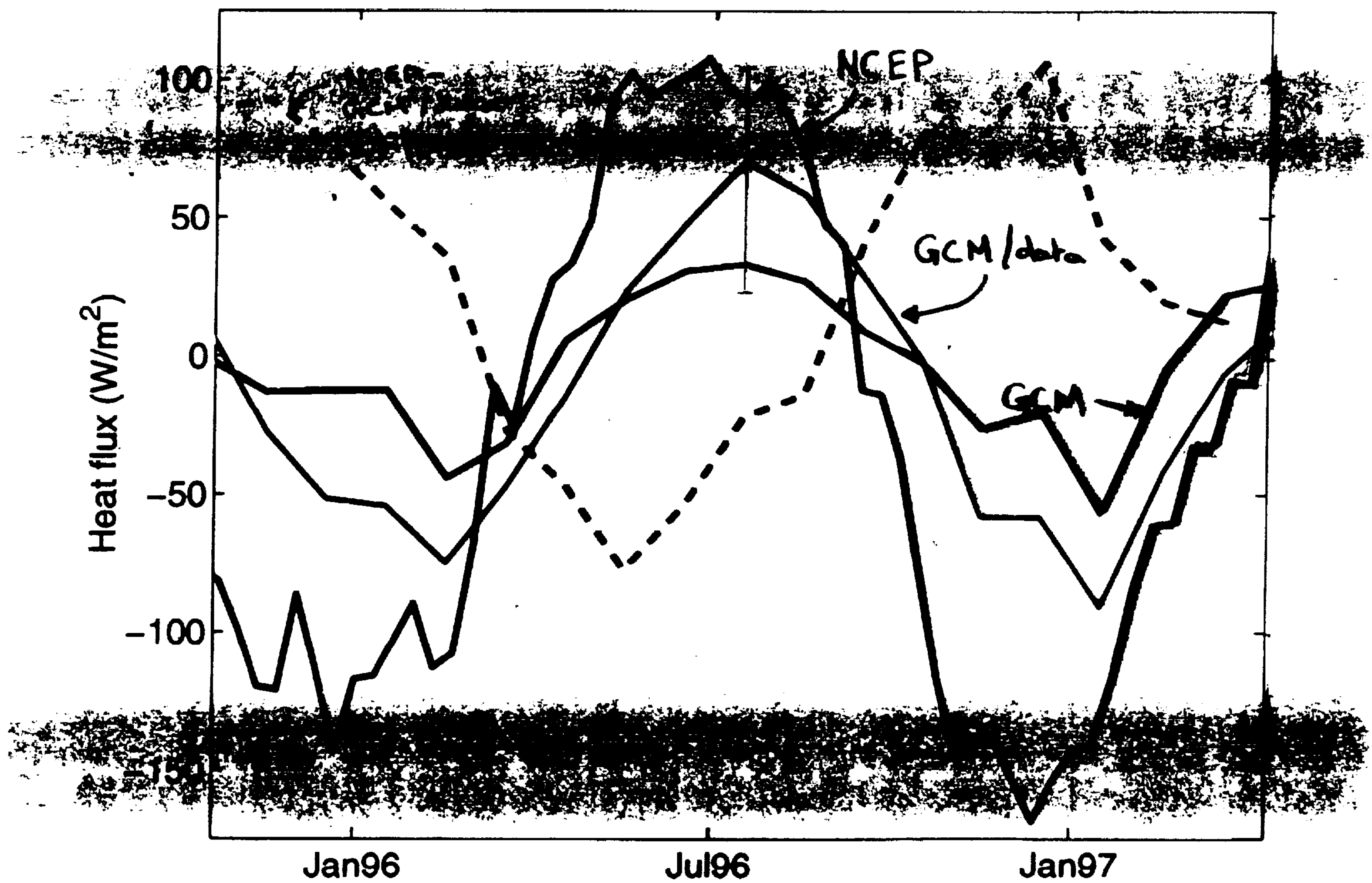

(ATOC Consortium '98)

Concluding Remarks

Acoustic tomography can be an effective data set for understanding [redacted]

Global ocean data assimilation system provides a framework for assimilating past and future ocean acoustic tomography data; it also provides boundary conditions for high resolution regional studies.

[redacted]

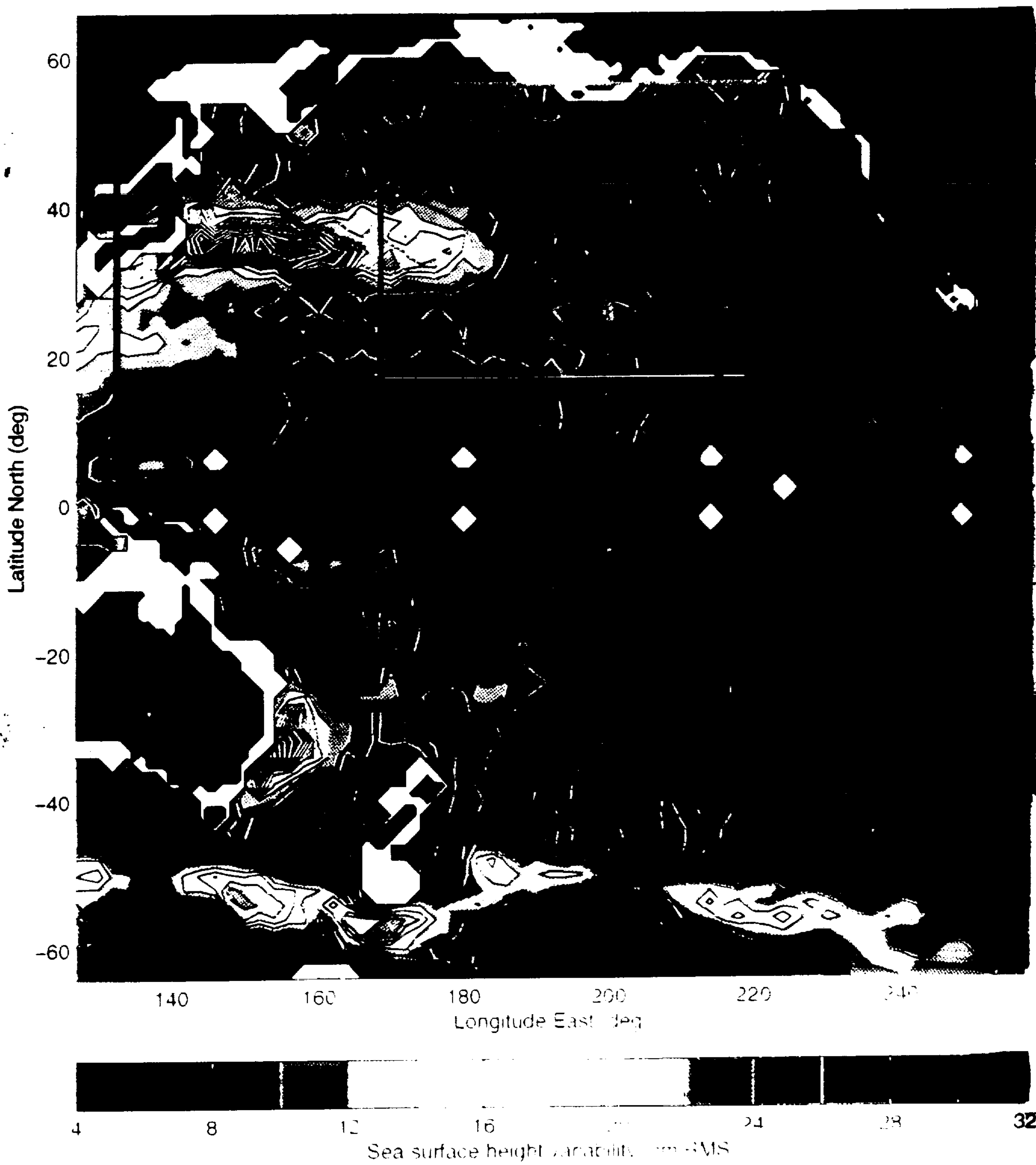
60
40
20
0
-20
-40
-60
Latitude North (deg)
140
160
180
200
220
Longitude East
4
8
16
32
Sea surface height

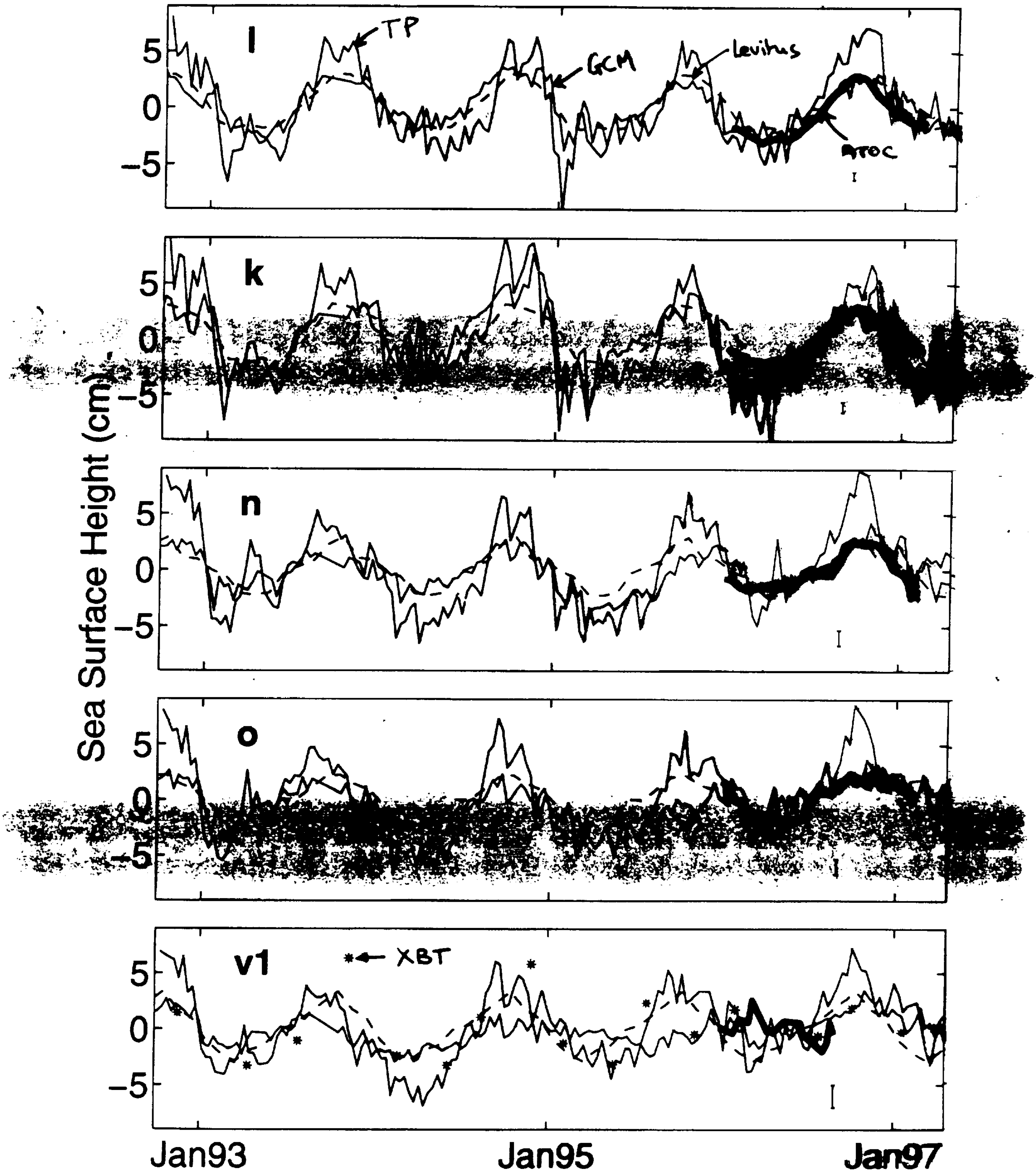

(The ATOC Consortium '98)